Showcasing research from the group of Dr Matthew Lloyd Davies, Applied Photochemistry Group (@Photochem_SU), SPECIFIC IKC, Materials Research Department, Swansea University, Wales, UK. The work was carried out in collaboration with Dr Peter Holliman, Swansea University.

Improving the light harvesting and colour range of methyl ammonium lead tri-bromide (MAPbBr$_3$) perovskite solar cells through co-sensitisation with organic dyes

Through the introduction of organic dyes into mesoporous MAPbBr$_3$ perovskite devices, we have highlighted the availability of 'space' within the device, which, when occupied by a dye can contribute to colourful and higher performing devices.

As featured in:

See Matthew L. Davies *et al.*, *Chem. Commun.*, 2019, **55**, 35.

ChemComm

Check for updates

Improving the light harvesting and colour range of methyl ammonium lead tri-bromide (MAPbBr₃) perovskite solar cells through co-sensitisation with organic dyes†

Tamara D. McFarlane,[a] Catherine S. De Castro, [ID][a] Peter J. Holliman [ID][b] and Matthew L. Davies [ID]*[a]

Co-sensitisation of methylammonium lead tri-bromide perovskite solar cells with red (D205) and blue (SQ2) organic dyes improves device efficiencies and allows device colour tuning. Sensitising the film after perovskite crystallisation produces higher device efficiencies (2.6% SQ2, 3.1% D205) than perovskite-only devices (2%) and devices sensitised before the perovskite layer deposition (1.5% SQ2, 2.0% D205).

Lead halide perovskites $(CH_3NH_3)PbX_3$ (X = Cl, Br or I) offer a versatile and performance effective photovoltaic (PV) material with current perovskite solar cell (PSC) efficiencies surpassing 22%.[1] Despite their progressive development, a principal limitation of these perovskites is their instability when exposed to ambient conditions.[2] Various studies have highlighted their sensitivity to: oxygen,[3] moisture,[4,5] light[6] and combinations of these factors.[7,8]

Additives introduced into the perovskite precursor solution can alter the perovskite morphology, a key factor in both device stability and performance.[9,10] Despite the sensitivity of perovskite thin-films to moisture,[11] studies have reported improved perovskite morphology through the introduction of small volumes of moisture to the precursor solutions of methyl ammonium lead iodide $(CH_3NH_3PbI_3/MAPbI_3)$[12,13] and methyl ammonium lead iodide/chloride $(CH_3NH_3PbI_{3-x}Cl_x/MAPbI_{3-x}Cl_x)$[14,15] perovskite. Believed to improve grain coverage[14] and limit pinholes,[12] moisture addition is thought to partially dissolve the perovskite (following formation) causing layer re-construction, which is thought to improve carrier lifetime and mobility.[15] Improvement of perovskite morphology has also been achieved through the addition of diiodo octane,[16,17] and chloronaphthalene[18] to the $MAPbI_{3-x}Cl_x$ perovskite precursor whereas $MAPbI_3$ devices have shown improvement with the addition of ammonium chloride,[19] 1,5-aminovaleric acid[20] and γ-butyrolactone[21] to the precursor solution.

Improvement in $MAPbI_3$ device performance (from 16.4 to 18.2%) and stability (only 7% degradation after ageing for 30 days) has also been reported through the addition of zinc chloride $(ZnCl_2)$ (to the precursor solution) which was attributed to improved grain size and morphology.[22] Similarly, better performance and stability of the $MAPbI_3$ perovskite layer has also been observed when doping the perovskite precursor with lithium salts. Increases from 11.3% to 18%, 17% and 15.6% were observed when including 1-butyl-3-methylimidazolium iodide, lithium iodide and bis(trifluoromethane)sulfonimide lithium salt in the perovskite precursor solutions, respectively.[23]

Treatment of the crystalline perovskite layer following formation has also proven to be beneficial. Noel *et al.* reported reduced hysteresis and non-radiative carrier recombination through treatment with thiophene and pyridine.[24] A similar effect was also observed when treating the perovskite layer with iodopenta-fluorobenzene which aided the passivation of trap states.[25]

Here, we report the treatment of the methyl ammonium lead tri-bromide $(CH_3NH_3PbBr_3/MAPbBr_3)$ perovskite with organic sensitising dyes in an attempt to colour tune devices, improve the light harvesting range and ultimately improve device performance.

$MAPbBr_3$ is relatively stable compared to $MAPbI_3$ due to higher binding energy and the smaller Bohr radius of bromide[26,27] however, $MAPbBr_3$ has a wider bandgap limiting the light harvesting efficiency.[28]

The use of one or more complimentary dyes (*i.e.* dyes that absorb in different areas of the visible spectrum) adsorbed to titania in a single device has proved to be successful in improving the efficiency of dye sensitised solar cells (DSSC).[29–31] Kakiage *et al.*[32] reported higher photovoltaic performance (14.3% efficiency) for DSSC's co-sensitised with ADEKA-1 (silyl-anchor dye) and LEG4 (carboxy-anchor dye) in comparison to a DSSC which used ADEKA-1 only (12.5% efficiency).[33]

An efficiency of 12.3% was also achieved by Yella *et al.*[34] through the combination of zinc porphyrin dyes, YD2-o-C8 and Y123.

[a] *Applied Photochemistry Group, Materials Research Centre, SPECIFIC IKC, Swansea University, Bay Campus, Fabian Way, Crymlyn Burrows, Swansea, SA1 8EN, UK. E-mail: M.l.davies@swansea.ac.uk*

[b] *CEMEG-Swansea (Chemistry Engineering Materials Environment Group) Materials Research Centre, SPECIFIC IKC, Swansea University, Bay Campus, Fabian Way, Crymlyn Burrows, Swansea, SA1 8EN, UK*

Presently, the highest reported efficiency for a MAPbBr$_3$ device (10.4%) was achieved through adding hydrogen bromide to the perovskite precursor.[36] MAPbBr$_3$ device efficiencies are generally lower than alternative lead halide perovskite systems where current leading device efficiencies of 22.1%[1] have been achieved using a formamidinium lead iodide/MAPbBr$_3$ perovskite. However, for co-sensitisation, the increased stability and relatively wide band gap (2.3 eV) of MAPbBr$_3$ allows extended device monitoring and separation of the dye and perovskite responses, which is ideal for studying the contribution of the dye in the device.

Paek et al.[35] have demonstrated the use of squaraine-based polymers as alternative hole transporting materials (HTMs) to spiro-OMeTAD in CH$_3$NH$_3$PbI$_3$ devices. These squaraine-based HTM's improved the light harvesting in the red region of the spectrum producing a slightly lower but comparable efficiency to control devices with spiro-OMeTAD.

Here, we demonstrate that organic dyes can be introduced into a mesoporous perovskite device and contribute to light harvesting thereby improving device performance. As a proof of concept, co-sensitisation has been investigated using the indoline dye, D205 and squaraine dye, SQ2 (ESI,† Fig. S1). These dyes absorb light in the green and red region of the visible spectrum allowing the dye uptake to be optically characterised. Interestingly, while 'hero' co-sensitised devices show improved short-circuit current and generally show an improvement over non-sensitised devices, improvement in the fill factor (FF) appears to be an important parameter for improved device efficiencies. Increases in FF are believed to result from both the dye solvent (toluene) and the dye, which are thought to improve the active layer homogeneity, further highlighting the benefits of treating the perovskite layer with a dye solution.[37]

The semi-transparent light orange colour of the MAPbBr$_3$ films allows for visualisation of the dye uptake (Fig. 1). There is an evident colour change of the active layer following sensitisation in the dye solution producing green and orange/red devices with SQ2 and D205 respectively. This highlights the potential for tuning the colour of PSCs yielding aesthetically attractive devices which could be advantageous for applications as building integrated PV, product-integrated PV or in tandem devices.

Absorption spectroscopy (Fig. 2) measurements confirm the presence of dye in the device and its contribution to the photocurrent.

Two methods were investigated to determine the effect of co-sensitising the films at different stages of device fabrication. The 'dye before' (DB) method involves dying the mesoporous

Fig. 1 Photographed thin films, left to right: control MAPbBr$_3$, solid state SQ2, MAPbBr$_3$ co-sensitised with SQ2 (MAPbBr$_3$/SQ2), solid state D205, MAPbBr$_3$ co-sensitised with D205 (MAPbBr$_3$/D205). * Solid state films were prepared on fluorine doped tin oxide glass (FTO) coated with mesoporous titania and dyed with D205 (FTO/TiO$_2$/D205) and SQ2 (FTO/TiO$_2$/SQ2).
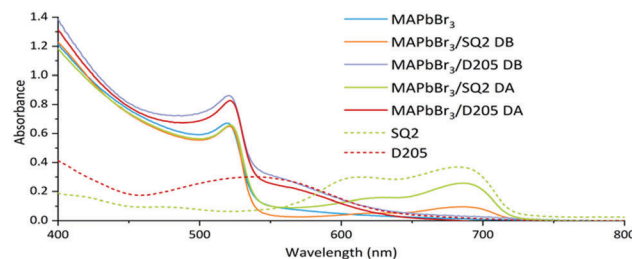

Fig. 2 Absorption spectra of control MAPbBr$_3$ devices, MAPbBr$_3$ devices co-sensitised with SQ2 and D205 using the DB method (MAPbBr$_3$/SQ2 DB and MAPbBr$_3$/D205 DB, respectively) and MAPbBr$_3$ devices co-sensitised with SQ2 and D205 using the DA method (MAPbBr$_3$/SQ2 DA and MAPbBr$_3$/D205 DA, respectively). The dashed lines represent solid state dyed films of D205 and SQ2.

titania layer prior to perovskite deposition, whereas the 'dye after' (DA) method involves soaking the crystallised perovskite film in the dye solution (see ESI† page 3 for full method).

Fig. 3 compares the efficiencies (PCE) of devices prepared using both the DA and DB method. An average PCE of 1.7% was observed with control MAPbBr$_3$ devices whereas DB devices co-sensitised with SQ2 and D205 showed a decrease in average PCE (1.3% and 1.1%, respectively). Devices co-sensitised using the DA method showed increased average PCE values of 2.1% and 2.3% with SQ2 and D205 respectively (ESI,† Table S2).

The DB method potentially hinders perovskite formation as the dye occupies space on the TiO$_2$ surface which would otherwise be available to the perovskite thereby reducing the PCE. We believe, the DA method allows the dye to occupy any unused space on the titania surface allowing the colour to be tuned while increasing the overall photocurrent and improving the fill factor of the device via solvent treatment.

PCEs of devices made using the DB method (Table 1) show lower device performance and decreased short-circuit current (J_{sc}).
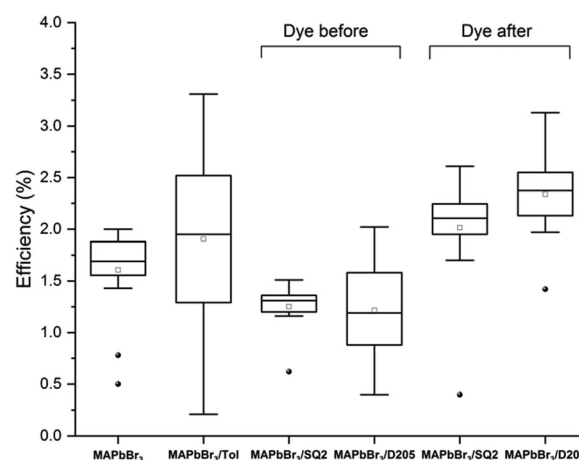

Fig. 3 Box plots of PCE (%) for control MAPbBr$_3$ devices, MAPbBr$_3$ devices submerged in toluene, MAPbBr$_3$ devices co-sensitised with SQ2 and D205 using the dye before method, and MAPbBr$_3$ devices co-sensitised with SQ2 and D205 using the dye after method. Each box plot is generated from at least 16 counter-electrodes 'pixels' (8 pixels per device) the full data set is available in the ESI,† Table S1.

Table 1 Measured photovoltaic performance values for the highest performing 'hero' pixel of control MAPbBr$_3$ devices, MAPbBr$_3$ devices co-sensitised with SQ2 and D205 using the dye before method (MAPbBr$_3$/SQ2 DB and MAPbBr$_3$/D205 DB, respectively) and MAPbBr$_3$ devices co-sensitised with SQ2 and D205 using the dye after method (MAPbBr$_3$/SQ2 DA and MAPbBr$_3$/D205 DA, respectively), when irradiated under 1 sun (100 mW cm^{-2}). Also included are the EQE generated short-circuit current values (EQE J_{sc}) for the hero pixel for each system

Device ID	EQE J_{sc} (mA cm^{-2})	J_{sc} (mA cm^{-2})	V_{oc} (V)	FF (%)	PCE (%)
MAPbBr$_3$	4.24	4.49	0.79	56	2.0
MAPbBr$_3$/SQ2 DB	2.93	3.18	0.85	55	1.5
MAPbBr$_3$/D205 DB	2.23	3.08	0.98	67	2.0
MAPbBr$_3$/SQ2 DA	4.85	4.80	0.75	72	2.6
MAPbBr$_3$/D205 DA	5.36	4.84	0.89	72	3.1

The observed increase in the open-circuit voltage (V_{oc}) may result from reduced recombination however, the EQE results (Fig. 5) show that little/no dye remains in the system. It is likely that the dye degrades during the annealing of the perovskite layer limiting the effectiveness of the DB method.

When comparing the PV performance values of the hero MAPbBr$_3$ device and the hero devices co-sensitised using the DA method, there is an increase in the J_{sc} (Table 1) for both SQ2 and D205. An increase in J_{sc} through co-sensitisation would typically be expected (as observed for the hero pixels) however, this is not always the case (ESI,† Tables S1 and S2) suggesting that there is a fine balance in maximising the dye response whilst not reducing the photocurrent generated from the perovskite. The aim is to simply 'top-up' the photocurrent, improve the device efficiency and have greater colour control.

While increases in photocurrent are not always seen upon the addition of the dye(s) the PCE's of the co-sensitised devices (using the DA method) are higher than non-sensitised devices. The hero devices co-sensitised using the DA method show an increased FF (Table 1) compared to the control devices and the same trend is found for the average FF values for the complete data set (Fig. 4).

These increases may, in part, be attributed to the solvent, toluene. Previously, toluene has been shown to increase overall performance when used as an anti-solvent treatment to aid the rapid crystallisation of CH$_3$NH$_3$Pb(I$_{1-x}$Br$_x$)$_3$ (x = 0.1–0.15) perovskite.[37] Denser films with improved uniformity and efficiency were reported.[37] In this study, MAPbBr$_3$ films soaked in toluene for 10 minutes resulted in some devices with a high FF and a slightly higher average FF than control devices (Fig. 4, MAPbBr$_3$/Tol) but overall show a higher degree of variability. Larger average increases in FF were observed with the dye solutions, suggesting that both the dye and solvent contribute to a higher FF and therefore PCE for MAPbBr$_3$ films co-sensitised using the DA method.

External quantum efficiency (EQE) measurements were performed on the hero pixels to determine the contributions of the dye and perovskite to the photocurrent. The EQE response of the hero MAPbBr$_3$ device reaches maximum at 380 nm and remains above 50% up to 520 nm. For hero devices co-sensitised using the DA method, the EQE results (Fig. 5) follow the same trend but also show an additional contribution (approximately 10%) of photocurrent over 550–750 nm range. These results prove that the dyes are harvesting incident photons within this wavelength range and contributing to the overall device photocurrent. Contrastingly, we observe a very low signal, and therefore poor charge injection, from the dye when studying the EQE spectra of the DB devices, thought to result from degradation of the dye following annealing of the perovskite layer. The reduction in the perovskite signal (300–550 nm) also supports the theory that the DB method affects perovskite formation, potentially by reducing the space available within the mesoporous layer.
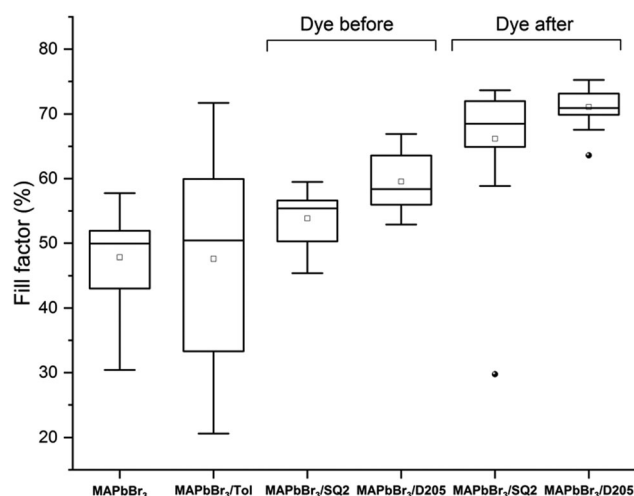

Fig. 4 Box plots of average FF (%) for control MAPbBr$_3$ devices, MAPbBr$_3$ devices submerged in toluene, MAPbBr$_3$ devices co-sensitised with SQ2 and D205 using the DB method and MAPbBr$_3$ devices co-sensitised with SQ2 and D205 using the DA method.
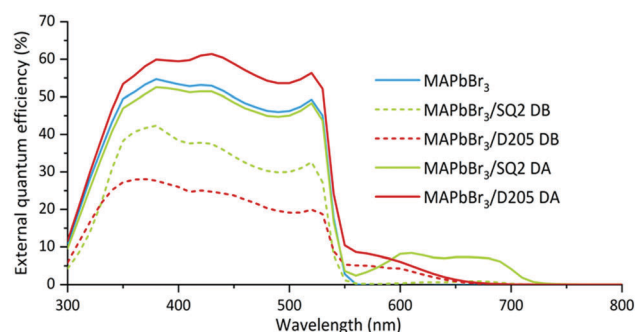

Fig. 5 Measured EQE spectral response for the hero pixel of control MAPbBr$_3$, MAPbBr$_3$ co-sensitised with SQ2 and D205 using the DB method (MAPbBr$_3$/SQ2 DB and MAPbBr$_3$/D205 DB, respectively) and MAPbBr$_3$ co-sensitised with SQ2 and D205 using the DA method (MAPbBr$_3$/SQ2 DA and MAPbBr$_3$/D205 DA, respectively).

We have demonstrated the possibility of colour tuning PSC's providing an improved aesthetic appeal which could be beneficial for building integrated photovoltaics and/or tandem photovoltaic systems. Devices co-sensitised using the 'dye-after' method (where the film is sensitised after annealing the perovskite) have demonstrated overall increased performance. This initial series of investigations has shown that co-sensitisation of MAPbBr$_3$ devices with organic dyes not only allows for colour alteration of the active layer but can also improve the device efficiency. Further optimisations are needed to balance maximising the response from the dye without hindering the performance of the perovskite material. We have highlighted that there is 'space' available within a perovskite device that could potentially be utilised to achieve higher performing and colourful devices. Additionally, there is a slight benefit from the dye solvent, toluene, but the data is less consistent than when a dye is present and it is unable to replicate the co-sensitised results indicating that there is synergistic benefit from both the dye and the solvent.

Conflicts of interest

There are no conflicts to declare.

Notes and references

1 W. S. Yang, B. W. Park, E. H. Jung, N. J. Jeon, Y. C. Kim, D. U. Lee, S. S. Shin, J. Seo, E. K. Kim, J. H. Noh and S. Il Seok, *Science*, 2017, **356**, 1376–1379.
2 M. Grätzel, *Nat. Mater.*, 2014, **13**, 838–842.
3 D. Bryant, N. Aristidou, S. Pont, I. Sanchez-Molina, T. Chotchunangatchaval, S. Wheeler, J. R. Durrant and S. A. Haque, *Energy Environ. Sci.*, 2016, **9**, 1655–1660.
4 J. M. Frost, K. T. Butler, F. Brivio, C. H. Hendon, M. Van Schilfgaarde and A. Walsh, *Nano Lett.*, 2014, **14**, 2584–2590.
5 J. Yang, B. D. Siempelkamp, D. Liu and T. L. Kelly, *ACS Nano*, 2015, **9**, 1955–1963.
6 T. Leijtens, G. E. Eperon, S. Pathak, A. Abate, M. M. Lee and H. J. Snaith, *Nat. Commun.*, 2013, **4**, 2885.
7 G. Niu, W. Li, F. Meng, L. Wang, H. Dong and Y. Qiu, *J. Mater. Chem. A*, 2014, **2**, 705–710.
8 G. Niu, X. Guo and L. Wang, *J. Mater. Chem. A*, 2015, **3**, 8970–8980.
9 G. E. Eperon, V. M. Burlakov, P. Docampo, A. Goriely and H. J. Snaith, *Adv. Funct. Mater.*, 2014, **24**, 151–157.
10 T. Salim, S. Sun, Y. Abe, A. Krishna, A. C. Grimsdale and Y.-M. Lam, *J. Mater. Chem. A*, 2014, **3**, 8943–8969.
11 J. Huang, S. Tan, P. Lund and H. Zhou, *Energy Environ. Sci.*, 2017, **10**, 2284–2311.
12 C.-G. Wu, C.-H. Chiang, Z.-L. Tseng, M. K. Nazeeruddin, A. Hagfeldt and M. Grätzel, *Energy Environ. Sci.*, 2015, **8**, 2725–2733.
13 K. K. Bass, R. E. McAnally, S. Zhou, P. I. Djurovich, M. E. Thompson and B. C. Melot, *Chem. Commun.*, 2014, **50**, 15819–15822.
14 J. You, Y. (Michael) Yang, Z. Hong, T.-B. Song, L. Meng, Y. Liu, C. Jiang, H. Zhou, W.-H. Chang, G. Li and Y. Yang, *Appl. Phys. Lett.*, 2014, **105**, 183902.
15 H. Zhou, Q. Chen, G. Li, S. Luo, T.-b. Song, H.-S. Duan, Z. Hong, J. You, Y. Liu and Y. Yang, *Science*, 2014, **345**, 542–546.
16 C.-C. Chueh, C.-Y. Liao, F. Zuo, S. T. Williams, P.-W. Liang and A. K.-Y. Jen, *J. Mater. Chem. A*, 2015, **3**, 9058–9062.
17 P. W. Liang, C. Y. Liao, C. C. Chueh, F. Zuo, S. T. Williams, X. K. Xin, J. Lin and A. K. Y. Jen, *Adv. Mater.*, 2014, **26**, 3748–3754.
18 X. Song, W. Wang, P. Sun, W. Ma and Z. K. Chen, *Appl. Phys. Lett.*, 2015, **106**, 033901.
19 L. Ding and C. Zuo, *Nanoscale*, 2014, **6**, 9935–9938.
20 A. Mei, X. Li, L. Liu, Z. Ku, T. Liu, Y. Rong, M. Xu, M. Hu, J. Chen, Y. Yang, M. Grätzel and H. Han, *Science*, 2014, **345**, 295–298.
21 H.-B. Kim, H. Choi, J. Jeong, S. Kim, B. Walker, S. Song and J. Y. Kim, *Nanoscale*, 2014, **6**, 6679.
22 J. Jin, H. Li, C. Chen, B. Zhang, L. Xu, B. Dong, H. Song and Q. Dai, *ACS Appl. Mater. Interfaces*, 2017, **9**, 42875–42882.
23 S. Mabrouk, B. Bahrami, A. Gurung, K. M. Reza, N. Adhikari, A. Dubey, R. Pathak, S. Yang and Q. Qiao, *Sustainable Energy Fuels*, 2017, **1**, 2162–2171.
24 N. K. Noel, A. Abate, S. D. Stranks, E. S. Parrott, V. M. Burlakov, A. Goriely and H. J. Snaith, *ACS Nano*, 2014, **8**, 9815–9821.
25 A. Abate, M. Saliba, D. J. Hollman, S. D. Stranks, K. Wojciechowski, R. Avolio, G. Grancini, A. Petrozza and H. J. Snaith, *Nano Lett.*, 2014, **14**, 3247–3254.
26 J. Knoester and V. M. Agranovich, *Thin Films Nanostruct.*, 2003, **31**, 1–96.
27 K. Tanaka, T. Takahashi, T. Ban, T. Kondo, K. Uchida and N. Miura, *Solid State Commun.*, 2003, **127**, 619–623.
28 K. Shankar, X. Feng and C. A. Grimes, *ACS Nano*, 2009, **3**, 788–794.
29 P. J. Holliman, M. L. Davies, A. Connell, B. V. Velasco and T. M. Watson, *Chem. Commun.*, 2010, **46**, 7256–7258.
30 M. L. Davies, T. M. Watson, P. J. Holliman, A. Connell and D. A. Worsley, *Chem. Commun.*, 2014, **50**, 12512–12514.
31 P. J. Holliman, M. Mohsen, A. Connell, M. L. Davies, K. Al-Salihi, M. B. Pitak, G. J. Tizzard, S. J. Coles, R. W. Harrington, W. Clegg, C. Serpa, O. H. Fontes, C. Charbonneau and M. J. Carnie, *J. Mater. Chem.*, 2012, **22**, 13318–13327.
32 K. Kakiage, Y. Aoyama, T. Yano, K. Oya, J. Fujisawa and M. Hanaya, *Chem. Commun.*, 2015, **51**, 15894–15897.
33 K. Kakiage, Y. Aoyama, T. Yano, T. Otsuka, T. Kyomen, M. Unno and M. Hanaya, *Chem. Commun.*, 2014, **50**, 6379–6381.
34 A. Yella, H. W. Lee, H. N. Tsao, C. Yi, A. K. Chandiran, M. K. Nazeeruddin, E. W. G. Diau, C. Y. Yeh, S. M. Zakeeruddin and M. Grätzel, *Science*, 2011, **334**, 629–634.
35 S. Paek, M. A. Rub, H. Choi, S. A. Kosa, K. A. Alamry, J. W. Cho, P. Gao, J. Ko, A. M. Asiri and M. K. Nazeeruddin, *Nanoscale*, 2016, **8**, 6335–6340.
36 J. H. Heo, D. H. Song and S. H. Im, *Adv. Mater.*, 2014, **26**, 8179–8183.
37 N. J. Jeon, J. H. Noh, Y. C. Kim, W. S. Yang, S. Ryu and S. Il Seok, *Nat. Mater.*, 2014, **13**, 897.